COMPARISON STUDY OF ASTRONOMICAL SITE QUALITY

OF MOUNT GRAHAM AND MAUNA KEA

K. Michael Merrill and Fred F. Forbes

National Optical Astronomy Observatories†
Advanced Development Program
P. O. Box 26732, Tucson, Arizona 85726-6732

with important contributions from:

L. D. Barr, J. Beckers, G. Favot, D. Morse, G. Poczulp, and L. Wallace

National Optical Astronomy Observatories†
P. O. Box 26732, Tucson, Arizona 85726-6732

March 17, 1987

PUBLIC RELEASE DATE: March 23, 1987

† Operated by the Association of Universities for Research in Astronomy, Inc., under contract with the National Science Foundation.

I. Introduction

The National Optical Astronomy Observatories (NOAO) is currently planning a ground-based 15-meter class optical/infrared National New Technology Telescope (NNTT). In conjunction with those plans, NOAO, together with the University of Arizona, the Smithsonian Astrophysical Observatory and the University of Hawaii, has also conducted a limited comparison of sites which might best permit the NNTT to achieve its full potential. Details of that survey are being published elsewhere by Forbes et al. and Merrill et al. (*SPIE Proceedings* **628**, pp. 118 and 125, 1986 and *NNTT Technology Development Program Report No. 11*, NOAO, Tucson, 1987). Where other sources are used, they will be cited specifically.

Since the NNTT will have as its most outstanding characteristic a high sensitivity at high angular resolution, especially in the thermal infrared, the prime site characteristics tested were seeing and infrared atmospheric emissivities. Secondary characteristics measured were near-ground turbulence, wind velocity, and temperature gradients. Important other characteristics such as speckle lifetime, isoplanatic patch size, and infrared sky noise were not part of the original measurements. The sites to be compared were selected with the preconditions of minimum sky brightness and distance from major cities.

Two sites have been tested: Mt. Graham in Arizona and Mauna Kea in Hawaii. They are briefly described in Section II. The equipment set up at the two sites consisted of a Seeing Monitor (SM) system, an Infrared Sky Radiance Monitor (ISRM) system, an Echosonde acoustic sounder and a Microthermal and Meteorological (M/M) tower. A description of the instrumentation, the duration of the tests, the data reduction procedures and the results are given in Section III. The results of the various measurements are summarized in Section IV.

II. The sites

According to Woolf and Merrill (1984, *Technology Development Program Report No. 4*; NOAO, Tucson), the combined requirements of low water vapor, clear sky and minimal artificial illumination led to Mauna Kea (elevation 13,800 feet, 4200 m, latitude +19°50′) as an obvious candidate, against which other potential sites should be judged. However, it was not known whether Mauna Kea was consistent with the needs of the NNTT or if a continental site might be as, or more, appropriate. Such considerations led to the selection of the Mt. Graham summit (High Peak) (elevation 10,700 feet, 3300 m, latitude +32°41′) as a second site to be included in the survey.

II.1 Mt. Graham

Mt. Graham is in the Pinaleño Mountains of southern Arizona and is part of the Coronado National Forest. It is located 115 km ENE of Tucson and 330 km WNW of El Paso. The closest community is Safford, Arizona (1970 population 6000). There is good road access to the site, only the last 5 miles requiring a 4-wheel drive vehicle. The site, which is covered with spruce-fir forest and is essentially undeveloped, is currently being considered by the University of Arizona as a potential site for telescopes. Since Mt. Graham is a new, undeveloped site, Kitt Peak, Mt. Lemmon and Mt. Hopkins have been used as proxy sites when needed for longer term experience.

The mean annual precipitation at the summit of Mt. Graham is 90cm, of which 60% is snow. At Fort Grant, which is 7 miles SW of the site, 50% of the annual precipitation falls between July and September when moist air flows in from the SE. On encountering the Pinaleño Mountains the air is forced to rise and become unstable and release its energy in moderate to violent thunderstorms in the late afternoon and evening. The remaining precipitation falls from October to March and is usually associated with storms moving in from the Pacific Ocean.

II.2 Mauna Kea

Mauna Kea is a dormant volcano on Hawaii and its peak is the highest point in the state. The summit is about 41 km WNW of Hilo (1970 population 26,000). It is reached over 11 miles of 4-wheel-drive dirt road from Hale Pohaku, the mid-level support facility, which in turn is approximately 35 miles over paved roads from either Hilo or Waimea. The site has been developed by the University of Hawaii and many telescopes are already in place.

The dominant factor in Hawaiian weather is the strength and persistence of the high pressure cell in the northeast Pacific ocean and its associated air stream known as the trade winds. The trade winds are associated with moist, well mixed air below the inversion layer (at approximately 2000m) and clear, dry, and non-turbulent air above the inversion. Between November and April the high pressure cell is displaced periodically by cyclonic storms from temperate latitudes. This enhances cloud cover and humidity at the summit of Mauna Kea. The mean annual precipitation at the summit of Mauna Kea is ~15 cm, most of which falls as snow during the winter.

III. Strategy, Location and Time Span

The basic strategy was to obtain concurrent, synoptic, comparative observations at each site using the same measuring equipment, observational techniques, and data analysis. In this way most or all of the systematic errors in the measurements are identical, minimizing their effects on the comparison. Image quality was tracked with the Seeing Monitor wherein the relative motion of two images was monitored with a dual-aperture telescope on a 10-meter seeing tower. Infrared sky background was measured with an Infrared Sky Radiance Monitor which gave direct measures of sky brightness in four bands, from near the top of the seeing towers. Cloud cover, temperature, wind velocity, relative humidity, etc., were measured as part of the survey and extracted from

other sources. Thermal turbulence near the ground was measured from a 30-meter Microthermal and Meteorological (M/M) tower and at intermediate levels (to $\sim$ 100 meters) with an Echosonde acoustical sounder.

The equipment was set up at the summit of Mt. Graham (High Peak) and on Puu Kea Ridge (Summit Ridge) between the University of Hawaii 88-inch telescope (UHT) and the CFHT on Mauna Kea. A schematic layout of the primary instrumentation at the sites is given in Figure 1.

On Mt. Graham measures of visual sky condition and infrared quality were begun in March 1984; Seeing Monitor measurements were begun in May 1985 and the Echosonde was put into operation in August 1985. On Mauna Kea measures of visual sky condition and infrared quality were begun in February 1984; the SM observations were started in December 1984 and Echosonde observations were initiated in March 1984. The survey terminated in December 1985 on Mauna Kea and in March 1986 on Mt. Graham.

III.1 Cloud Cover, Relative Humidity, Temperature Variations and Winds

Cloud cover. Three measures of visible cloud cover were made. Visually clear (VCLR) is defined as times when no visible clouds were reported. This is meant to be analogous to "photometric". Sky OK (SKYOK) is defined as times when the cloud cover was $\leq$ 6/10 and intermittent. This is meant to be analogous to "spectroscopic" and includes VCLR. The final category is suitable for astronomy (SFA). This required cloud cover as for SKYOK, with the additional requirements of no fog or precipitation, a maximum relative humidity, RH_{max}(e.g., $\sim$ 95%) and a maximum wind velocity, V_{max} (e.g., 40 mph) at low elevations (6 m at Mauna Kea and 15 m at Mt. Graham). An infrared criterion is discussed in §III.3.

Figure 1

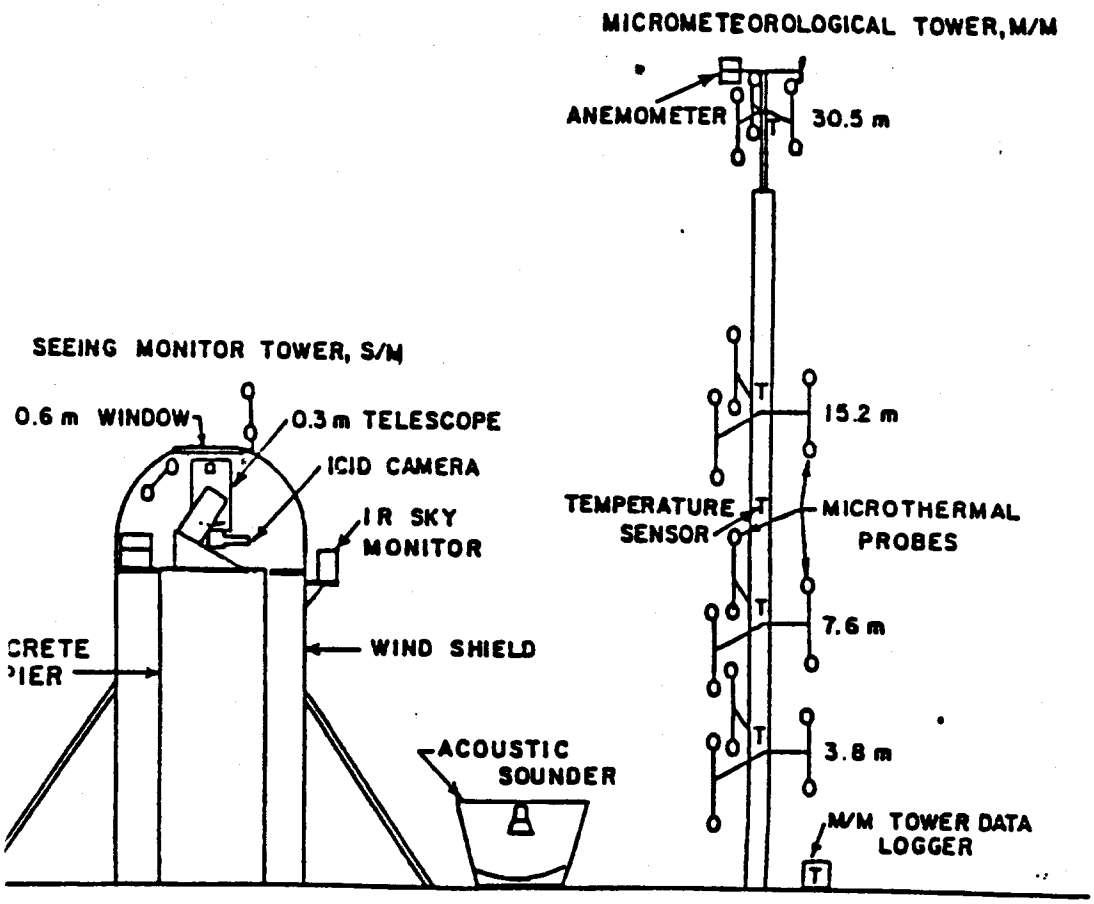

1. Schematic layout of the primary instrumentation deployed at Mt. Grad Mauna Kea for the Site Evaluation Project.

Figure 2

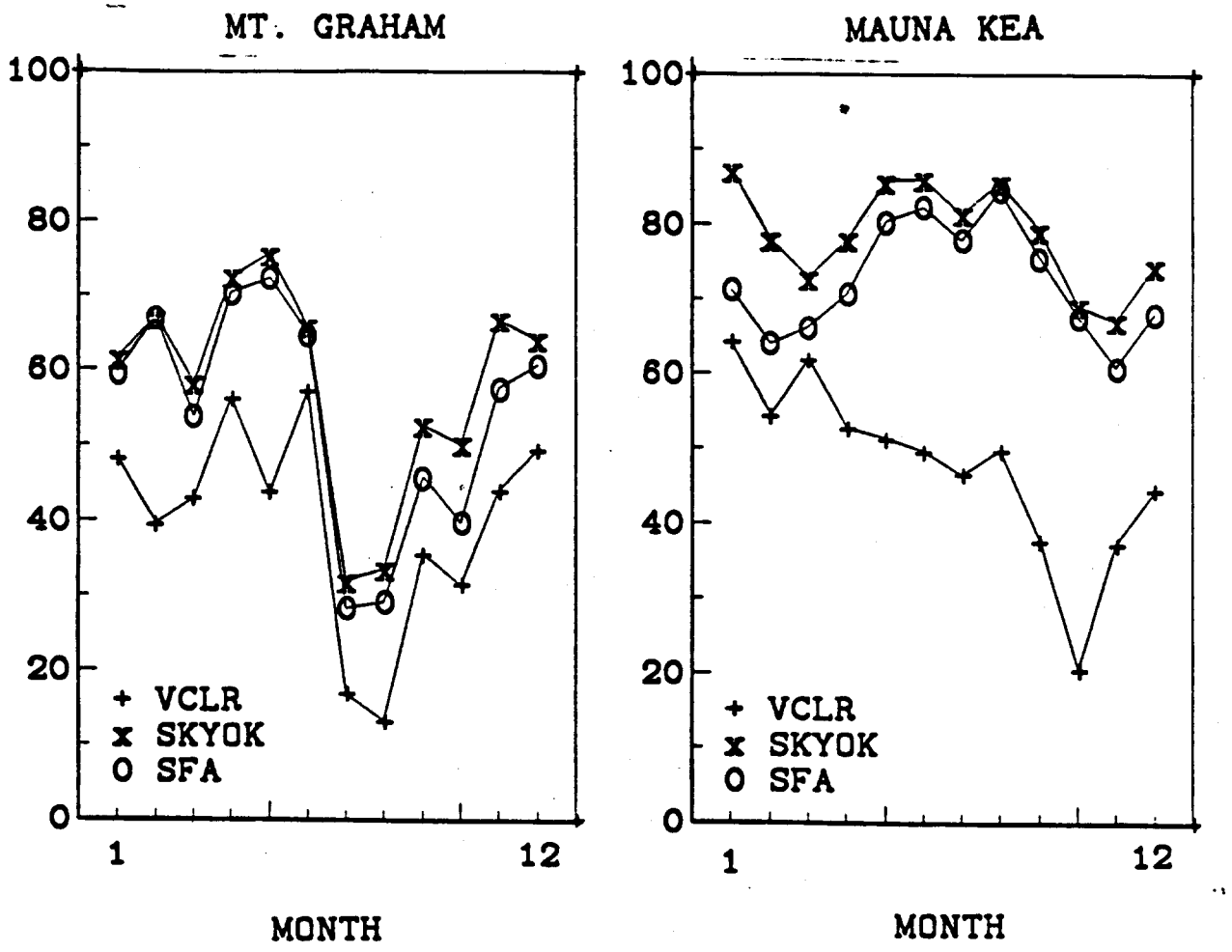

Figure 2. Percentage of time for Mt. Graham and Mauna Kea when sky conditions were visually clear (VCLR), OK (SKYOK), and suitable for astronomy (SFA).

A summary of the survey data by month, expressed as a percentage of the available time with data (for RH_{max} = 95% and V_{max} = 40 mph), is given in Figure 2. Variations in these maximum values result in only small changes. For Mt. Graham, the very poor conditions in July and August, which are a result of the monsoon season, are a prominent feature. For the total time period, the condition VCLR occurred 41% of the time, SKYOK occurred 59% of the time and SFA occurred 54% of the time. By way of comparison, the annual mean percentage usable hours at KPNO for 1964-1986 was 69% compared to 66% for all of 1984-1986 and 64% for the specific months during 1984-1986 covered by our survey.

For Mauna Kea, the poor conditions in VCLR in October were caused by cirrus clouds. This is consistent with the expectation that cirrus would be most frequent in April and May and in October and November. For the total time period, VCLR occurred 48% of the time, SKYOK occurred 78% of the time and SFA occurred 73% of the time. These percentages can be compared to longer term values derived from UHT records for comparable quantities. On the basis of UHT observing logbook data summarized by Kaufman and Vecchione (1981, UC TMT Report No. 66), the mean percentage of usable hours with cloud cover <= 6/10 was 72% during 1970-1978, compared to our value of 78% SKYOK for 1984-1985. The UHT "trouble log", which tabulates actual time lost to observing, yields an annual mean of 74% usable hours for 1974-1985, compared to 77% for 1985-1985.

The results obtained at Mt. Graham are consistent with the experience at Kitt Peak and Mt. Lemmon. This is illustrated in part in Figure 3. Similarly the results for Mauna Kea are consistent with other data for Mauna Kea. The conditions during the time covered by the survey (horizontal bars) do not appear to be extraordinary.

Relative humidity. The monthly means, measured at 1 m elevation on Mt. Gra-

ham and from the 88-inch UHT catwalk on Mauna Kea, are shown in Figure 4. Mt. Graham, with a median value of 73%, is a much more humid site than Mauna Kea, which had a median value of 25%. This high humidity caused some loss of time in the SFA category for Mt. Graham and little for Mauna Kea. However, this loss of time is essentially equalized by a similar amount of time lost because of high winds on Mauna Kea which were not a substantial factor at Mt. Graham.

Temperature variations. The temperatures measured at the M/M towers, which were automatically recorded, have been analyzed in a number of different ways. The average diurnal range in temperature is important from the standpoint of thermal control of the telescope and its mirrors. It is small for both sites, amounting to $\sim 6\,^{\circ}$C for Mt. Graham and $\sim 4\,^{\circ}$C for Mauna Kea. The nocturnal temperature gradient is important for the thermal time constant of the mirrors and the mirror seeing. The measurements of this gradient are illustrated in Figure 5. The absolute value of the gradient is about the same for the two sites, with means of $\sim 0.3\,^{\circ}$C/hr and medians of $\sim 0.25\,^{\circ}$C/hr at a height of $\sim$12m above the ground. The material for the average nocturnal vertical temperature gradient is not available for the two sites for the same months, but the averages for Mt. Graham for the interval October through April is $0.07\,^{\circ}$C/m, while that for Mauna Kea for July and August is $0.02\,^{\circ}$C/m.

Winds. The near-ground winds are an important consideration in telescope construction. On Mt. Graham they were measured at 15m elevation, near or just above the tree-top level where the winds are still increasing upward to as much as a factor of 1.5 to 2 higher at 30m. On Mauna Kea (where there are no trees) they were measured at 6m and the wind is almost constant with altitude. The results are illustrated in Figure 6. The data for Mt. Graham indicate a mean wind speed of 12 mph and a dominant westerly direction. For Mauna Kea the mean wind speed was 16 mph and the direction was

ENE to ESE 37% of the time and WNW to WSW 36% of the time. If the data are restricted to nights considered suitable for astronomy (SFA), the mean speed for Mt. Graham is 12 mph and that for Mauna Kea is 14 mph.

High-level winds may be important for speckle lifetimes since much of the seeing may originate there. The monthly mean values obtained from Rawinsonde records for the time span of the survey are given in Figure 7. Since the high-level winds do not change rapidly with location, Tucson and Hilo should be good proxies for Mt. Graham and Mauna Kea. From the figure, it appears that there is not much difference between the two locations; the averages are 25 m/s for Tucson and 28 m/s for Hilo. The 22-year record, also given in Figure 7, indicates the survey period to be normal.

Figure 3

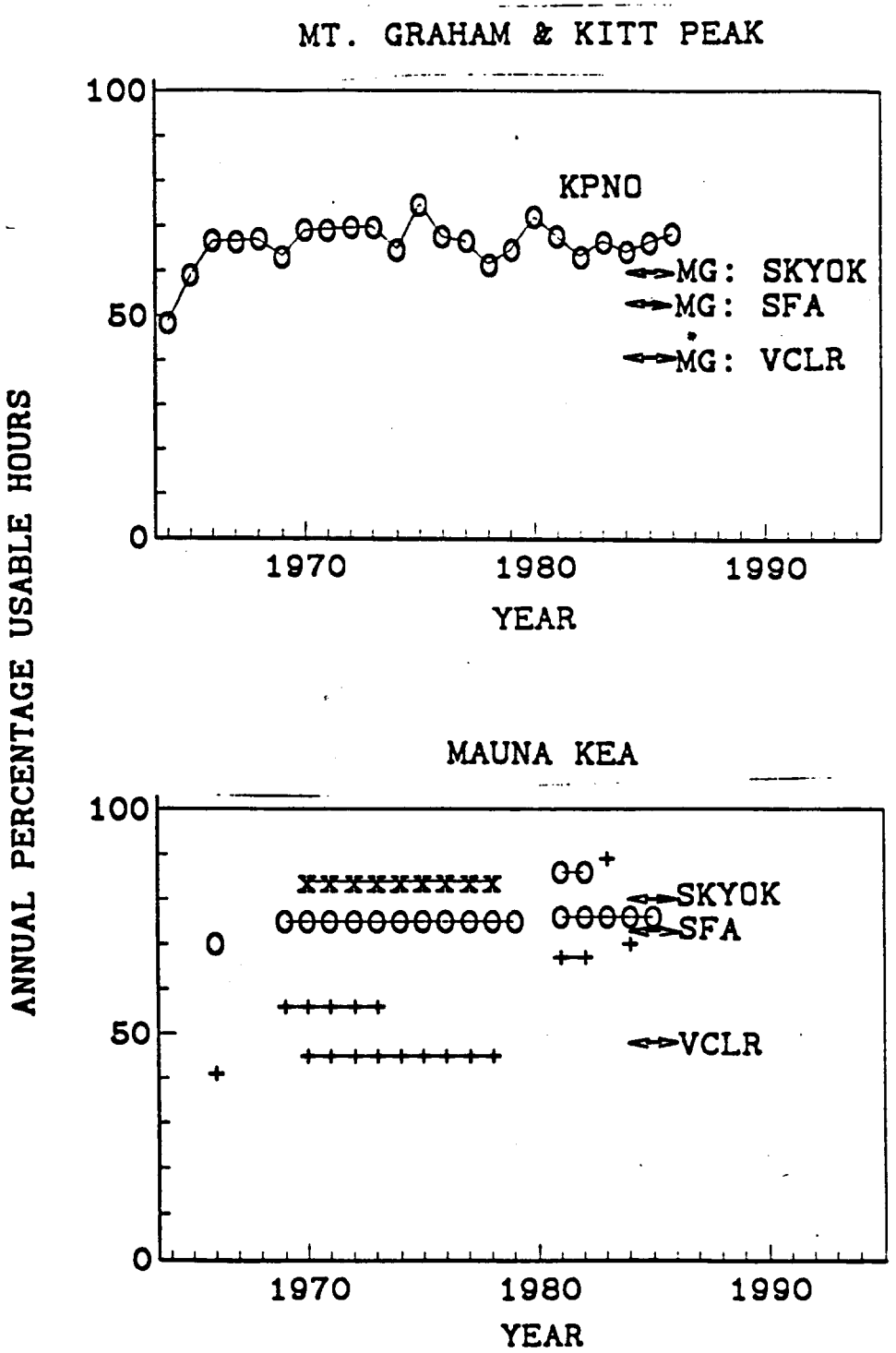

Figure 3. Comparison of Site Survey results, indicated by horizontal arrows, with the annual records for Kitt Peak and various averages over a period of years for Mauna Kea from surveys and log book summaries. The symbols +, × and o represent measures corresponding to VCLR, SKYOK and SFA as in the previous figure. Since several independent estimates for sky clarity exist for Mauna Kea, there are sometimes two estimates for a given year.

Figure 4

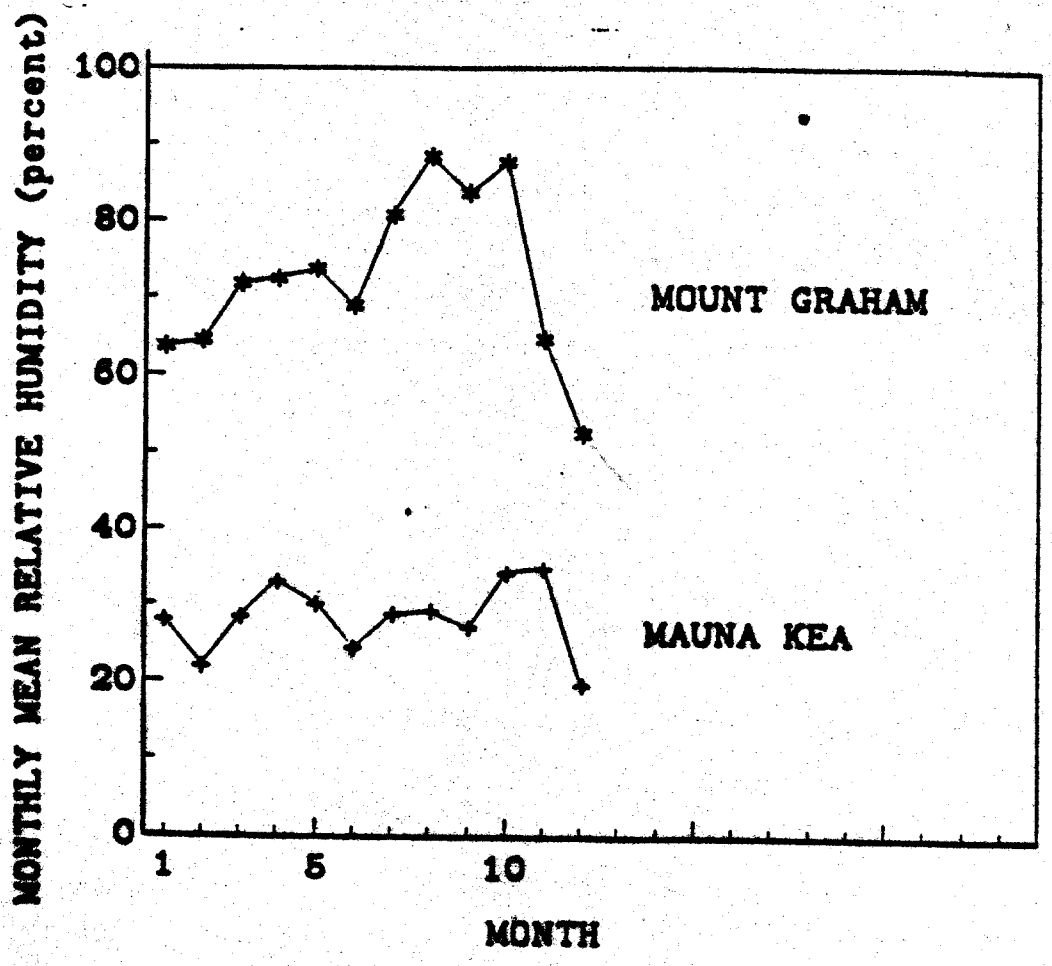

Figure 4. Monthly mean relative humidity for Mt. Graham and Mauna Kea.

Figure 5

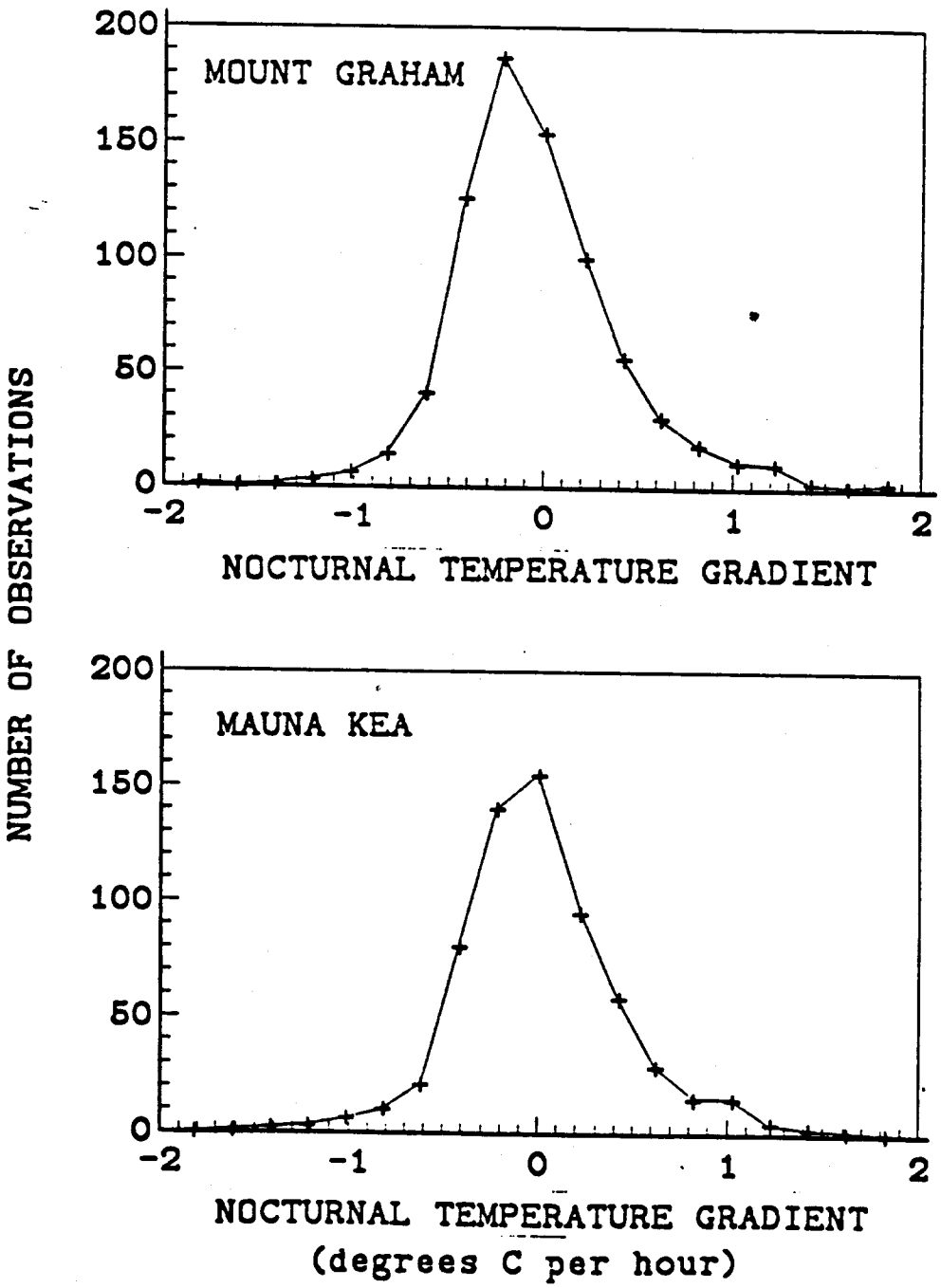

Figure 5. Nocturnal temperature gradients for Mt. Graham (764 measurements) and Mauna Kea (638 measurements).

Figure 6

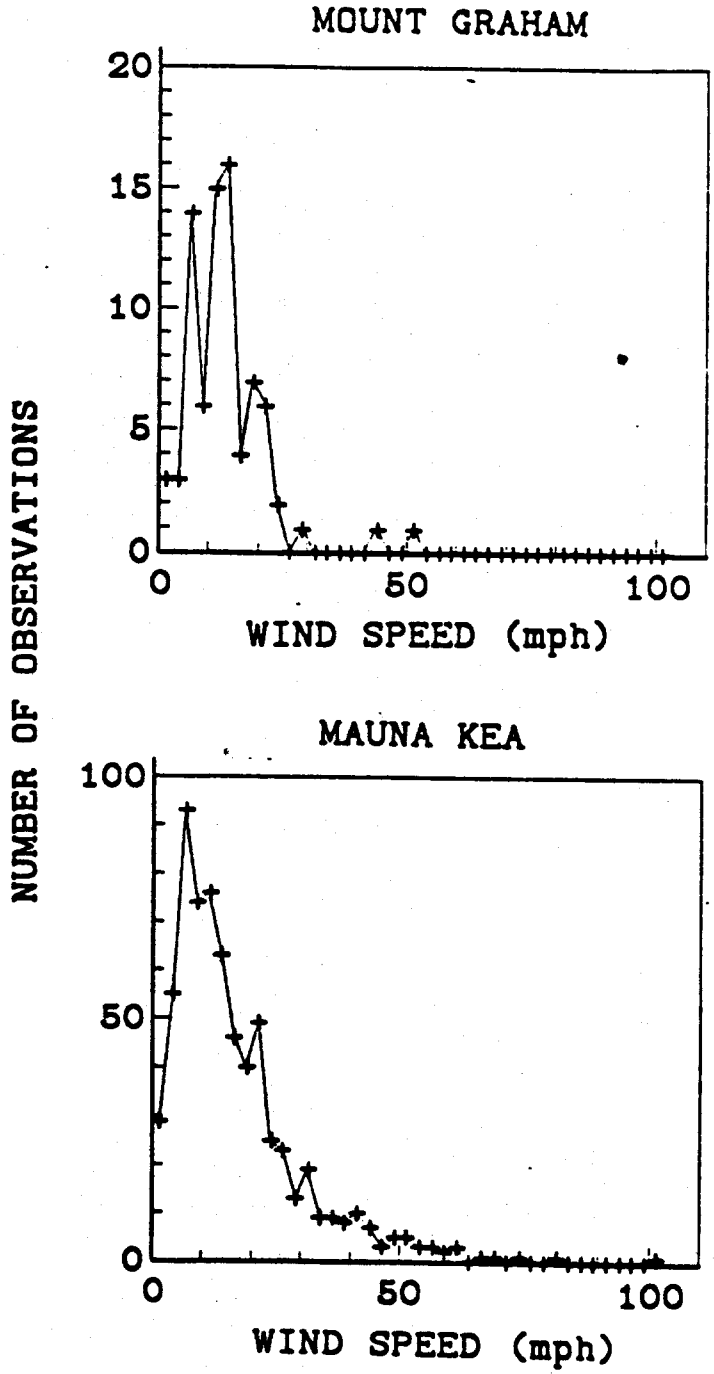

Figure 6. Low-level nightly mean wind speeds for Mt. Graham (78 nights) and Mauna Kea (677 nights).

Figure 7

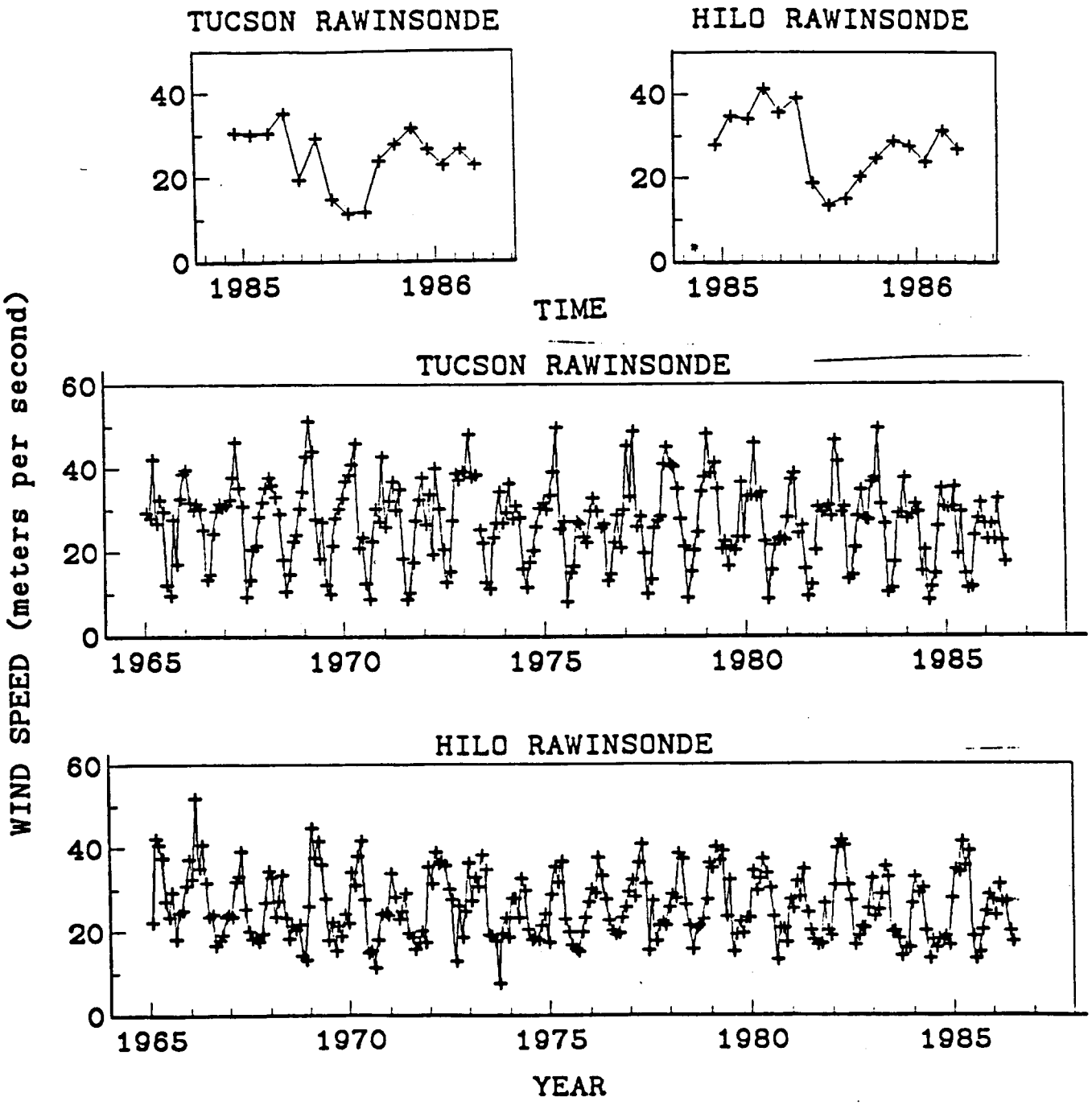

Figure 7. High-level monthly mean wind speeds from the Tucson and Hilo Rawinsonde records. These are the speeds at the 200 mb pressure level.

III.2 Seeing Monitor (SM) system

The optical arrangement is indicated in Figure 8. The instrument was designed primarily to measure the differential change in the separation between two images of a single star. A mask with two 10-cm diameter sub-apertures spaced 20 cm center-to-center was placed in front of the telescope with the holes aligned in right ascension. One of the apertures had an optical wedge in front of it so that two distinct images of the star were formed in the focal plane. The double-image technique eliminated tracking and vibration errors and the enclosure gave wind shielding. The 10-meter height of the isolated concrete pier avoided most of the ground-layer seeing.

The image data, recorded with an intensified CID camera at a 30-Hz frame rate, provided 47-second continuous records of 1/30-sec integrations of the dual image. In the analysis each 32×1 pixel image data slice, an example of which is given in Figure 8, was fitted with a seven-parameter profile consisting of two Gaussians and a constant background. From this fitting process, after correction for instrumental zero-point, the rms variation in image separation ($\Delta\alpha$) at temporal frequencies above 1 Hz was derived as the primary measure of seeing quality. The motions below 1 Hz were omitted because of the presence of an unexplained low frequency contribution.

Figure 9 gives the hourly means of the raw $\Delta\alpha$ values both including and excluding the 0-1 Hz temporal frequencies for the two sites. The results are quite different, Mt. Graham having the broader distribution with a median $\Delta\alpha$ (1-15 Hz) of 0.315 arcsec and Mauna Kea having the narrower distribution and a median observed $\Delta\alpha$ of 0.161 arcsec. The current dual-aperture observations have a shorter time constant than the previous photographic and visual observations used to test, for example, Mauna Kea and Mt. Hopkins. Even so, the time constant of 1/30 second is still long enough to filter out an appreciable amount of differential image motion particularily when the motion of the wavefront

(i.e., the wind velocity) is rapid.

Modeling of the wavefront structure by a Kolmogoroff spectrum shows that the typical E-W 13 m/s velocities (associated for example with the maximum jet stream layer shear region) reduce the true $\Delta\alpha$ values due to that layer by as much as 60%. Turbulence at even higher wind velocities (e.g. in the jet stream itself) would be virtually undetectable with the present dual aperture system. The lower wind velocities at near-ground levels ($\sim$ 5 m/s), and the not strictly E-W velocities will make the reduction in $\Delta\alpha$ by temporal filtering effects less but still significant ($\sim$ 25%). The corrections for the two sites are very similar since the wind velocities at the two sites are very similar (see § III.1). Differences in the correction factor could occur, due to differences in the relative contributions of the different heights to the seeing, and the direction of the wind.

We currently estimate the corrected median $\Delta\alpha$ values to be between 0.41 and 0.47 arcsec for Mt. Graham and between 0.21 and 0.30 arcsec for Mauna Kea. The lower value for each mountain assumes little or no contribution to the seeing of layers with wind speeds over $\sim$15 m/s, whereas the higher value includes a contribution of "undetectable seeing" at higher wind speeds ($>$ 15 m/s) which is assumed to be proportional to the 200 mb wind speed and which corresponds to 0.4 arcsec FWHM (close to the average contribution predicted for the entire free atmosphere) at a 200 mb wind speed of 25 m/s. We note that the corrections for the missing high frequency $\Delta\alpha$ motions are uncertain. There is also some uncertainty associated with the estimate of the motions present in the 0-1 Hz bandpass. We, however, do not believe that the uncertainties will change the sense of the differences (which favor Mauna Kea) either in the $\Delta\alpha$ values or in the image sizes which might be inferred.

Figure 8

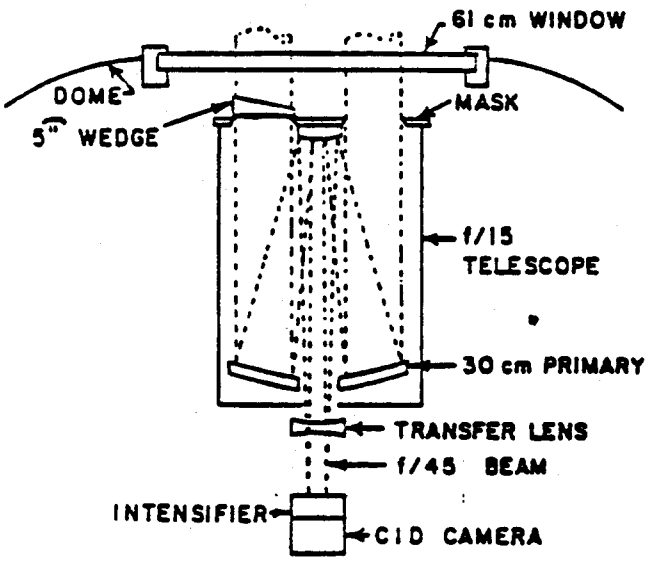

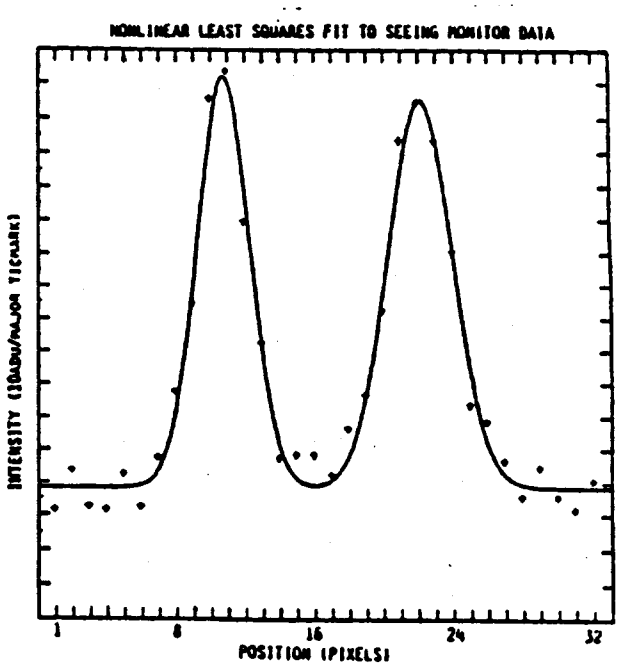

Figure 8. The upper panel shows the arrangement of the Seeing Monitor optical elements within the closed dome. The lower panel shows a representative least squares fit (solid curve) to the data (small + symbols) of a 32×1 pixel image frame from the Seeing Monitor.

Figure 9

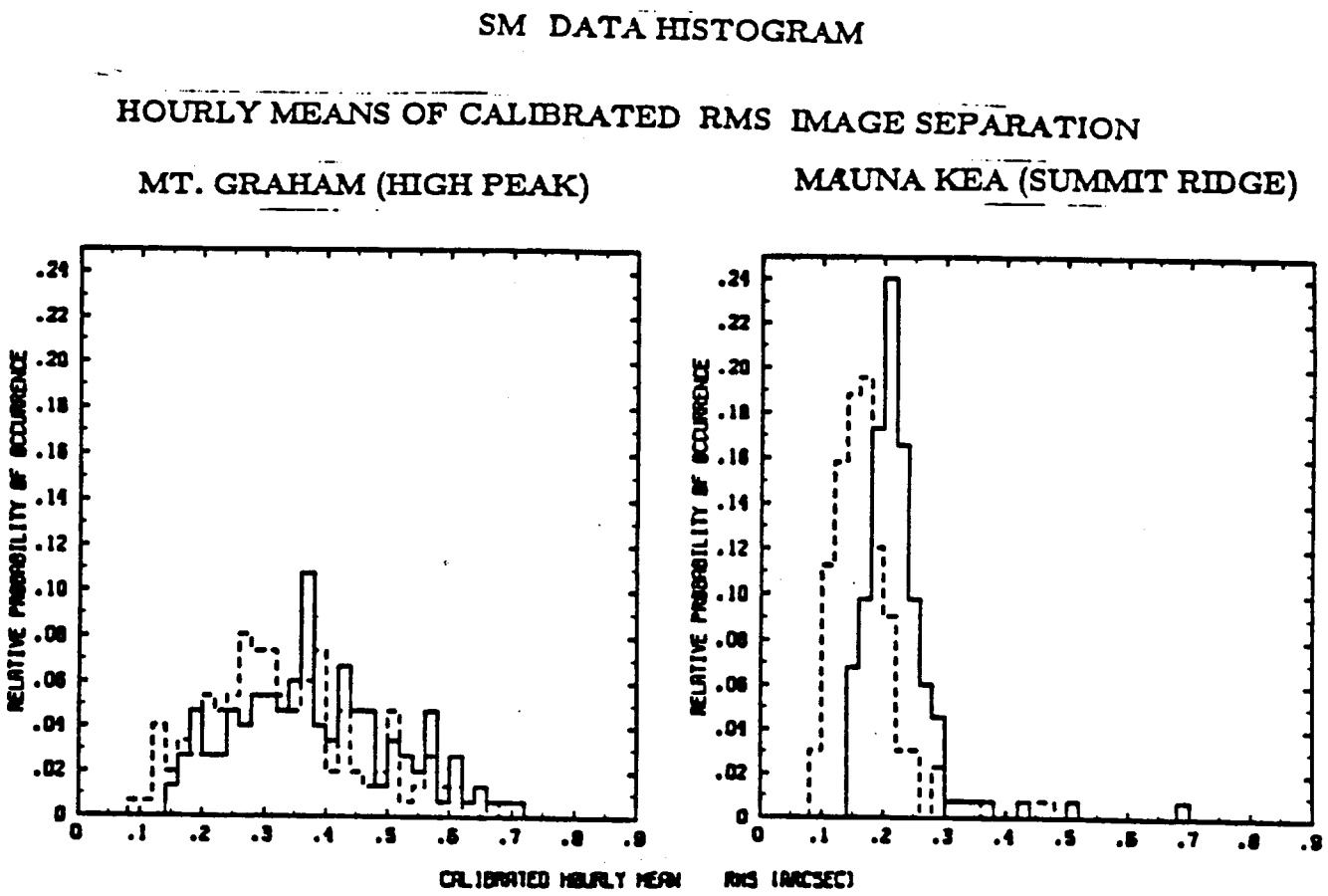

Figure 9. The RMS variation in image separation as obtained from the Seeing Monitor system. The full curves are for a bandwidth of 0-15 Hz and the dashed curves are for 1-15 Hz.

III.3 Infrared Sky Radiance Monitor (ISRM)

This instrument provided direct broad-band measurements of sky radiance through filters at 11, 15, 20 and 27μm. A schematic view of the instrument is given in Figure 10. The chopper wheel provides the detector with alternate views of the sky and an internal blackbody surface so that the output signal is proportional to the difference between the two sources. This difference signal was converted to sky radiance on the basis of a calibration with a liquid nitrogen temperature surface covering the field of view. These direct measurements were then converted to measurements of sky emissivity by ratioing with the blackbody flux at the sky temperature.

The 11-μm band has high transparency and is influenced primarily by cloud cover. By comparison with the meteorological records it was found that an 11-μm emissivity ($\epsilon_{11\mu m}$) of $\sim$ 0.08 separated times of high sky transparency from times of low transparency. This value was therefore used to define the times when infrared observations could have been made (IROK). The 15-μm band is opaque owing to CO_2 and was used in determining the sky temperatures, while the 20- and 27-μm bands are dominated by water vapor. The latter two can be used with a model of absorption by the water vapor lines to derive column amounts of water vapor, and to estimate the strength of water vapor lines as well as the emissivities at other wavelengths. That is done in *NNTT Technology Development Program Report No. 11* (1987: NOAO, Tucson), but for the present purpose of comparing the two sites for the NNTT the IR emissivities are the quantities of prime importance.

The statistics on the individual measurements of $\epsilon_{20\mu m}$ and $\epsilon_{27\mu m}$ at times when infrared observations could have been made, according to the 11-μm criterion, are given in Figure 11. The 20-μm distribution for Mt. Graham has a mean emissivity of 0.55 and a median of 0.54, while for Mauna Kea the mean is 0.36 and the median is 0.35. At 27

μm the distributions are more different, the one for Mt. Graham peaking between 0.975 and 1.000. The mean and median for Mt. Graham are 0.81 and 0.84 while the mean and median for Mauna Kea are both 0.67.

The monthly mean emissivities are given in Figure 12. The mean values of $\epsilon_{20\mu m}$ and $\epsilon_{27\mu m}$ were essentially the same at the two sites in November and December; at other months Mt. Graham showed a substantially higher emissivity than Mauna Kea.

A longer-term view of the infrared site characteristics has been reconstructed from Rawinsonde records, which in themselves constitute a useful pool of information on potential sites. The daily relative humidity data for Tucson and Hilo have been converted into water vapor density and integrated over height beginning at Mt. Graham altitude for the Tucson data and at Mauna Kea altitude for the Hilo data. The monthly mean results, given in Figure 13, should be good approximations to the water vapor amounts for the sites, barring substantial local effects. However, since relative humidities below 20% are not accurately recorded, archival Rawinsonde data may overestimate the water vapor under the driest conditions. The mid-year peak in the water vapor for Mt. Graham, which is the cause of the mid-year peak in the emissivities, is seen to be a persistent feature. The Mauna Kea record, on the other hand, shows a less pronounced maximum in October or November, which is also reflected in the emissivity measurements. From this long-term record, it does not appear that the survey period was in any way exceptional.

Figure 10

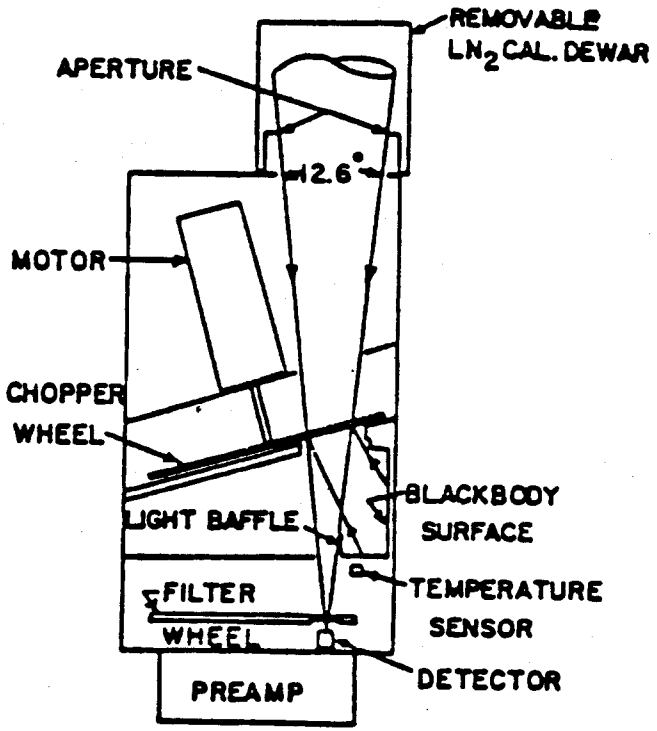

Figure 10. Schematic view of the Infrared Sky Radiance Monitor (ISRM).

Figure 11

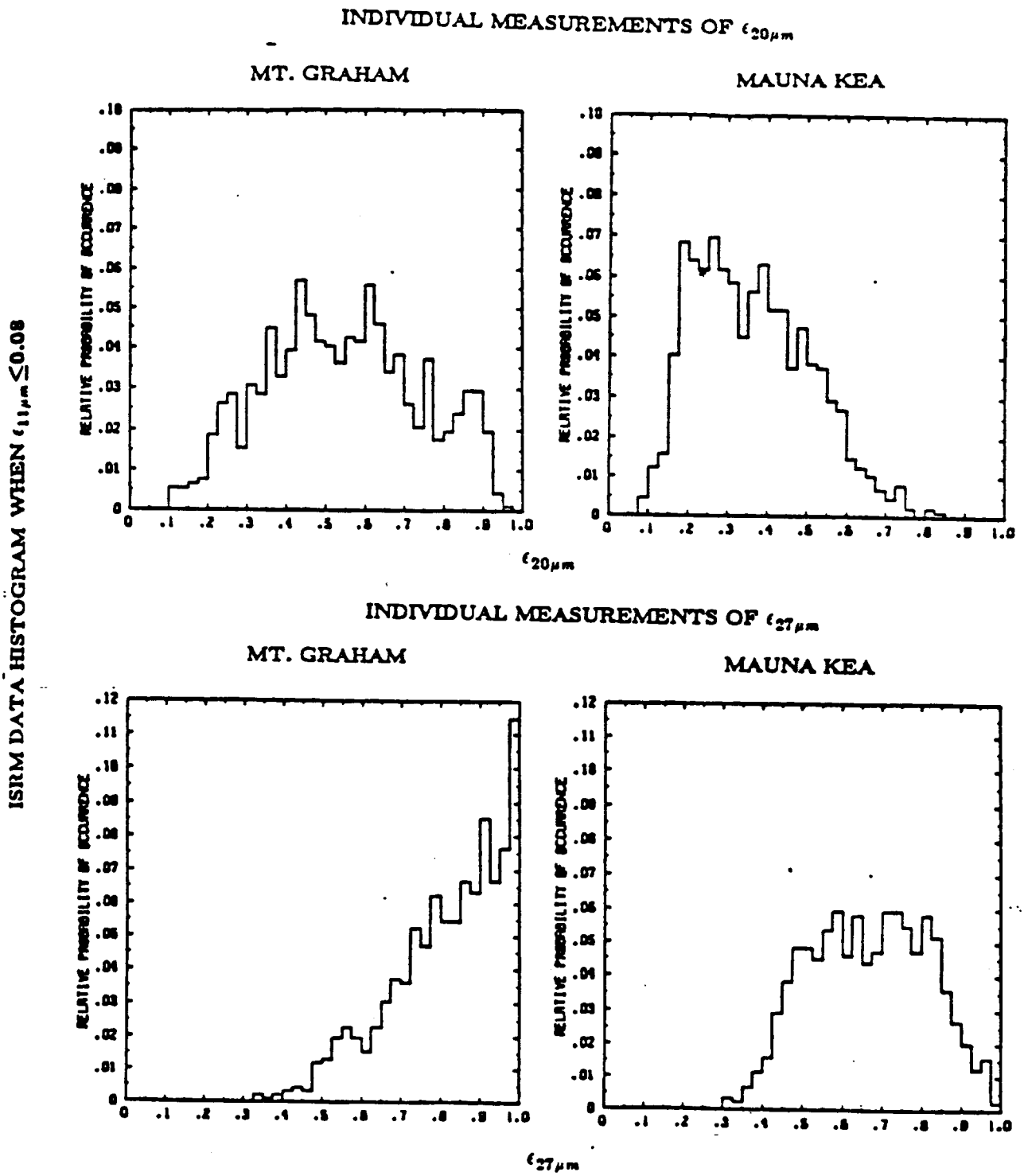

Figure 11. Individual measurements of sky emissivities at 20 and 27μm when the sky was IROK at Mt. Graham and Mauna Kea.

Figure 12

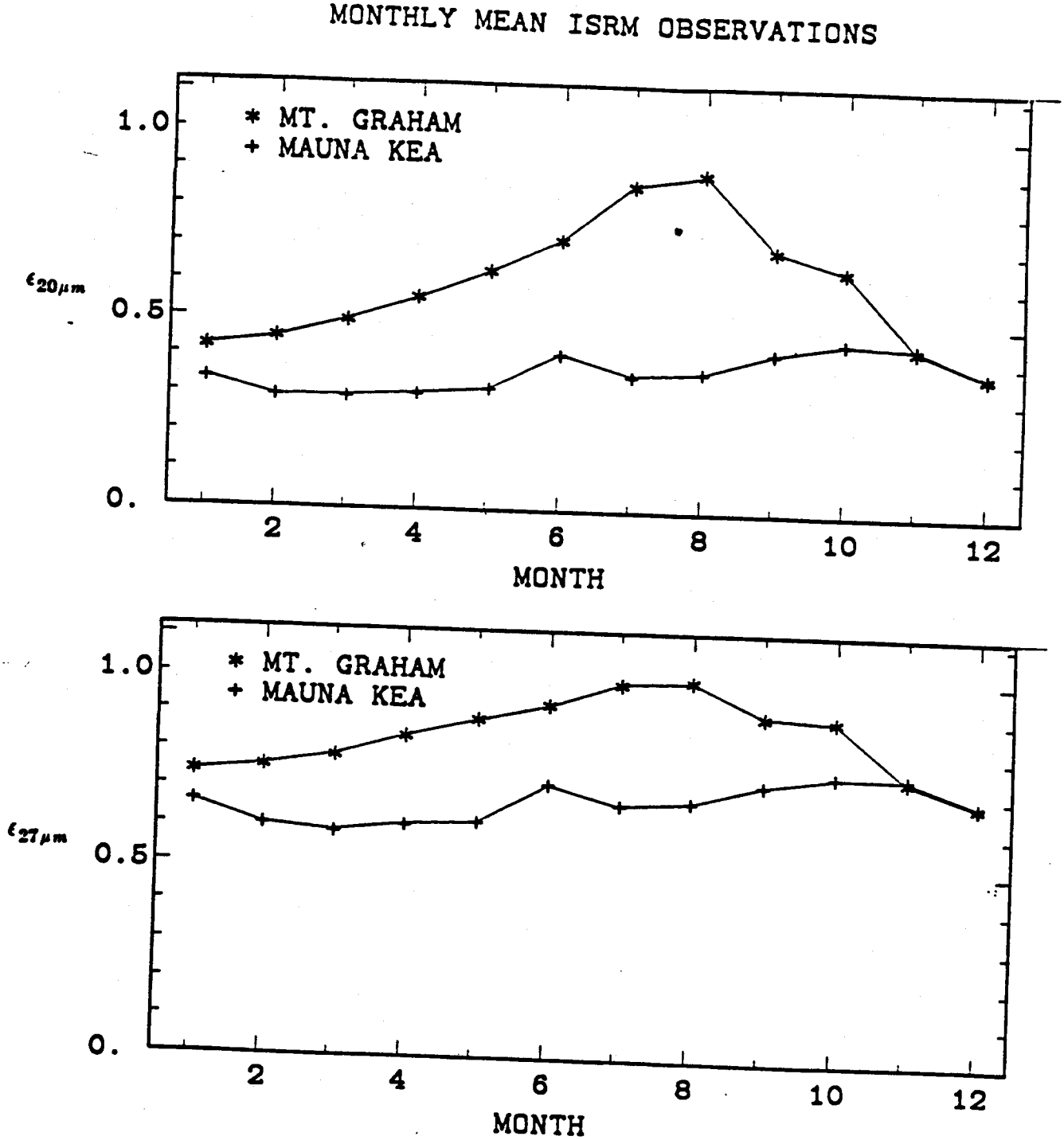

Figure 12. Monthly mean sky emissivities at 20 and 27μm for Mt. Graham and Mauna Kea.

Figure 13

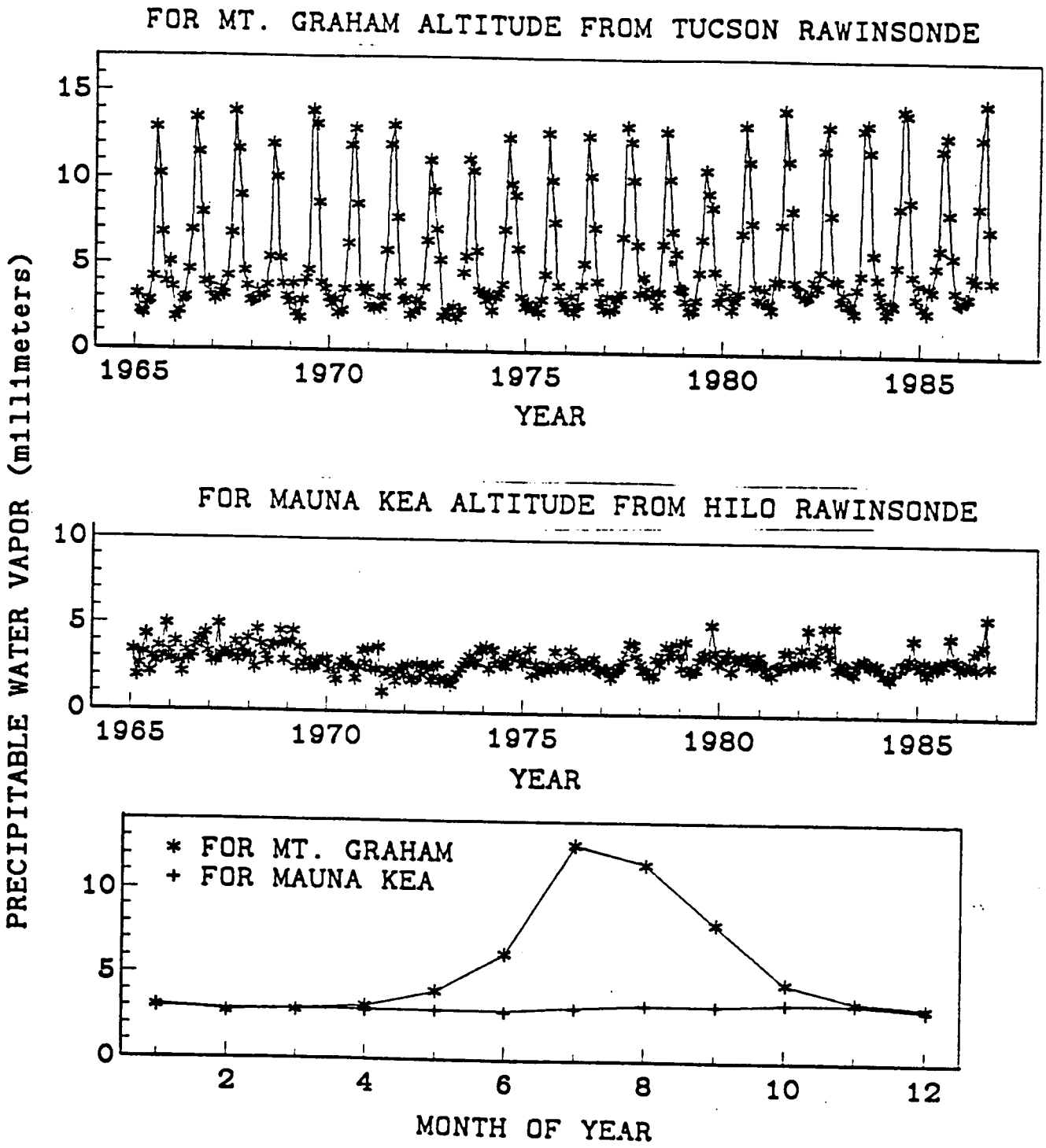

Figure 13. The top and center panels give the monthly mean water vapor amount for Mt. Graham and Mauna Kea from 1965 to 1986, in units of millimeters of precipitable water vapor calculated from Rawinsonde records. The lower panel gives the average by month for the same time span. Since relative humidities below 20% are not accurately recorded, archival Rawinsonde data may overestimate the water vapor under the driest conditions.

III.4 Thermal Turbulence Measurements from the Microthermal /Meteorological Towers

Maintenance of the microthermal sensors on the towers at both locations proved to be very difficult; the towers at both sites collapsed during winter storms more than once because of ice loading and winds. The data obtained are sparse. The instantaneous temperature differences were measured by the sensor pairs at three tower levels (see Figure 1) to provide data sets of 1520 values over 43 seconds. In the analysis each such data string was converted into a power spectral density distribution, corrected for extraneous noise, and integrated over frequency to obtain the atmospheric structure temperature parameter C_T^2.

The average results for the two sites are summarized in Figure 14. Since the data were not always available at all levels, the values represent different time averages. On Mauna Kea the results indicate a steady decrease of C_T^2 with height. The Mt. Graham results, on the other hand, are nearly constant with height and lower at low height than at Mauna Kea. This different character may be due to the influence of the trees on Mt. Graham.

III.5 Thermal Turbulence Measurements from the Echosondes

The Echosondes use the acoustic echo sounding technique. Pulses of acoustic energy at a fixed frequency are directed upward into the atmosphere at fixed time intervals. A small fraction of each pulse is scattered back by temperature fluctuations in the atmosphere and this backscattered signal is detected and recorded. A 1.5-m diameter antenna first transmitted a 2 KHz 10-degree conical signal of 50-ms duration, then switched to detect the backscatter for about 1 second, and repeated the cycle every 10 seconds.

In the analysis, the theory of electromagnetic and acoustic backscatter in a turbulent atmosphere is invoked to obtain C_T^2 from the recorded signal. Figure 14 shows

the Echosonde results for the two sites as well as the microthermal sensor measurements. The Echosonde data span a wider range of time than the microthermal results. The Echosonde values refer to heights of 16 to 80 meters, whereas the microthermal sensor measurements refer to lower heights. While the microthermal sensor values for Mt. Graham are less than or equal to those for Mauna Kea at low heights (below the tree tops on Mt. Graham), at greater heights C_T^2 on Mt. Graham exceeds the value for Mauna Kea by an order of magnitude. The flattening of the Mauna Kea curve above 40m is consistent with the level of instrumental noise, which increases with the square of the height.

Figure 15 shows the monthly and hourly variation of the Echosonde observations at a number of heights for nights designated SFA. The difference in C_T^2 between the sites is independent of the time of year. It is however quite different from the day-to-night-variation. C_T^2 for the two sites is almost the same during the day. The difference is pronounced only at night when C_T^2 drops a roughly a factor of 10 lower at Mauna Kea than the corresponding decrease at Mt. Graham.

Figure 14

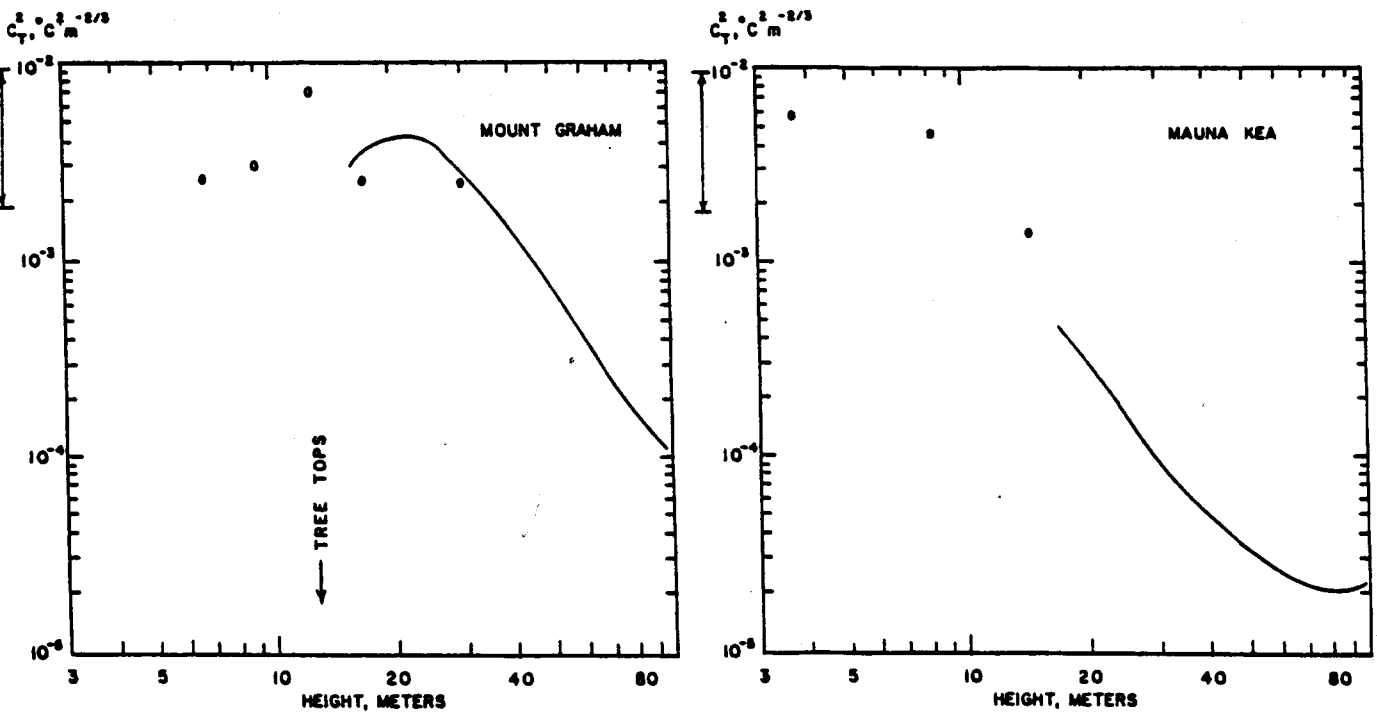

Figure 14. Logarithmic average C_T^2 versus height above the ground for microthermal (filled and open circles circles) and Echosonde (solid curves) data for Mt. Graham and Mauna Kea for nights designated SFA. The representative spread (25 to 75 percentile) for the data are indicated by the vertical bars on the left. The filled and open circles indicate data taken when the Mt. Graham M/M tower was deployed at different heights. The mean values for the open circles include approximately 10X as many observations as the values for the closed circles. The tree top height is shown in the upper panel for Mt. Graham.

Figure 15

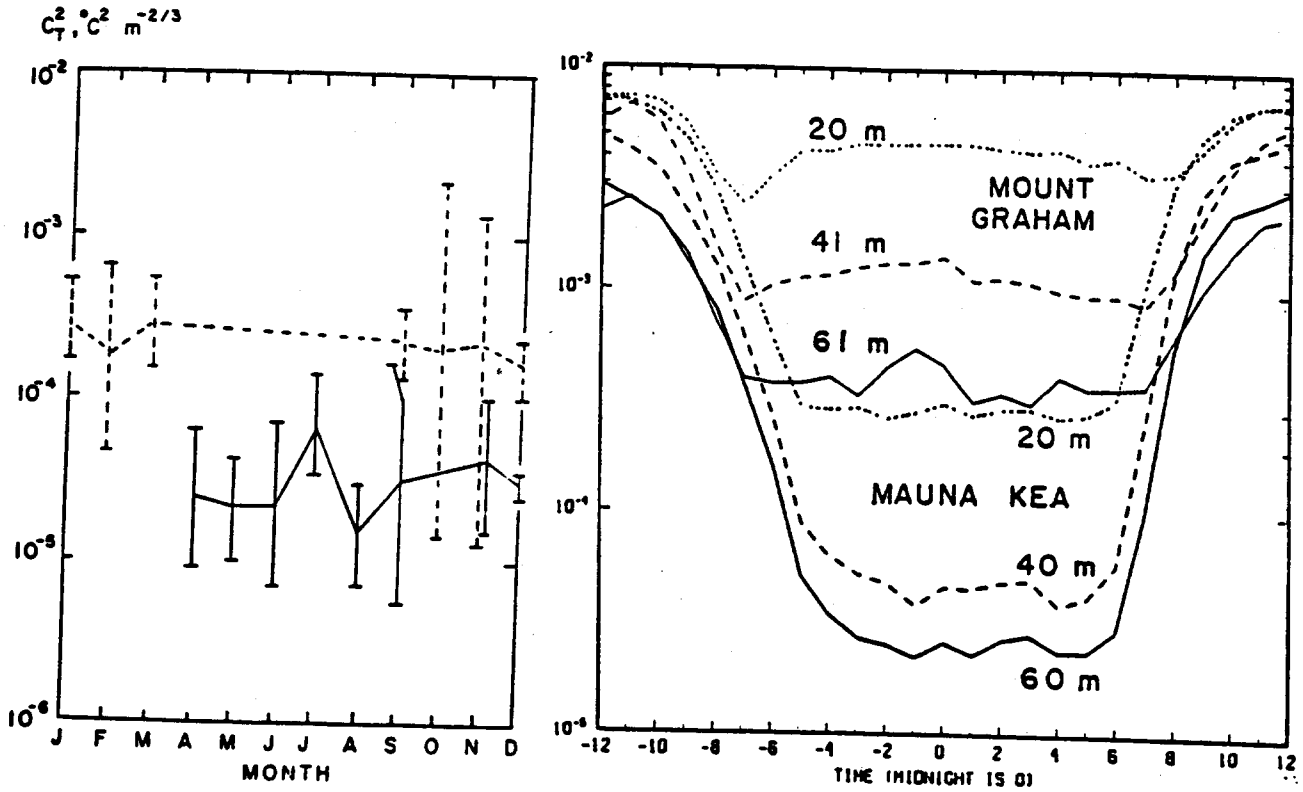

Figure 15. Mean monthly and hourly nighttime variation in C_T^2 at various heights above the ground for Echosonde data at Mt. Graham and Mauna Kea for nights designated SFA. The mean monthly C_T^2 averages at a height of 40 m above the ground for Mt. Graham (dashed) and Mauna Kea (solid) are shown on the left. The hourly C_T^2 averages at three heights are shown on the right.

IV. Summary

The table below summarizes the astronomical parameters for the two sites:

QUANTITY	MT. GRAHAM*	MAUNA KEA*
- ELEVATION:	3300 m	4200 m
- PRESSURE:	680 mb	616 mb
- LATITUDE:	+33°	+20°
- LONGITUDE:	110° W	155° W
- SKY CLARITY:		
Totally Clear Nights (VCLR)	41%**	48%**
Suitable Nights (SFA)	54%**/58%***	73%**/69%***
- RELATIVE HUMIDITY AT GROUND:		
50 percentile	73%	25%
- RMS IMAGE MOTION:		
50 percentile, uncorrected	0.31"	0.16"
50 percentile, corrected	0.41"-0.47"	0.21"-0.30"
- IR EMISSIVITY (%):	20μm 27μm	20μm 27μm
10 percentile	30% 62%	19% 47%
50 percentile	57% 86%	36% 69%
- NOCTURNAL TEMPERATURE:		
10 percentile	-4°C	-3°C**
50 percentile	2°C	2°C**
90 percentile	11°C	5°C**
- TEMPERATURE GRADIENT:		
Median During Night	-0.1 °C/hr	-0.1 °C/hr
Average Absolute Value	0.30 °C/hr.	0.30 °C/hr
- DAY/NIGHT T-DIFFERENCE:	6°C	4°C
- VERTICAL T GRADIENT:	0.07°C/m	0.02°C/m
- WIND VELOCITY:		
Median at Ground	5 m/s	7 m/s**
Median At Tropopause(200mb)	24 m/s**	25 m/s**

* Data refer to High Peak on Mt. Graham and the Summit Ridge on Mauna Kea.
** Long term averages available but not used to adjust data.
*** Long term averages used to adjust data.

In all respects, except for the microthermal activity near the ground, it appears therefore that Mauna Kea has the superior astronomical qualities needed for the National New Technology Telescope. In addition to these the Mauna Kea Site provides a larger sky coverage because of its latitude. Its latitude and climate allows, for example, the good study of the center of the Milky Way which transits at an elevation of 41° at midnight in June.

It is important that further studies of the NNTT site on Mauna Kea be undertaken to characterize it closer for design aspects of the NNTT and its instrumentation. Of particular interest are:

- a determination of the image FWHM that can be achieved with large telescopes. This is of particular importance for the image quality specifications of the NNTT. Our current $\Delta\alpha$ estimates infer a median FWHM at 550 nm in the range of 0.4"-0.6".
- an understanding of why present telescopes on Mauna Kea do not achieve this image quality.
- measurements of speckle lifetime and isoplanatic patch size. This is of importance for the adaptive optics design for the NNTT.
- measurement of the IR sky noise characteristics. This has a direct impact on the planning of IR instrumentation.

V. Acknowledgements

An effort with as wide a scope as the NOAO/NNTT Site Evaluation Project could not have happened without the dedicated effort of a large number of people.

J. T. Williams of the F. L. Whipple Observatory, Smithsonian Astrophysical Observatory, provided invaluable guidance and assistance in bringing the Mt. Graham site into operation. L. Thompson and N. J. Woolf, site scientists for Hawaii and Arizona respectively, provided continued critically needed support and advice. Special thanks are given K. Shu, G. Toures and B. Harris at NOAO for the design and the execution of much of the equipment. We all gratefully acknowledge the Herculean efforts of the site observers, D. Jacobson, J. Pomeroy, and E. Wolgemuth at Mauna Kea, and D. Officer and P. Welch, at Mt. Graham, during the unstinting performance of their duties. The support staffs at Mauna Kea, the Institute for Astronomy, and Steward Observatory provided logistic support throughout the Project. The authors wish to acknowledge extensive discussions with J. Jefferies, C. R. Lynds, and F. Roddier at NOAO and A. Erasmus at the University of Hawaii. We gratefully acknowledge critical comments for a variety of people during preparation of this manuscript, notably: P. A. Strittmatter, J. R. Angel, F. J. Low, B. Martin, R. Martin, and G. Rieke from the University of Arizona; D. N. B. Hall, E. Becklin, L. Cowie, A. Erasmus, and J. P. Henry from the University of Hawaii; and the members of the Hoag Committee - A. A. Hoag, R. D. Gehrz, J. P. Huchra, R. G. Kron, and H. A. McAlister. J. Goad at NOAO and G. Plasch at the Institute for Astronomy have provided invaluable editorial assistance throughout.

KMM gratefully acknowledges the continued support of his wife Boosik and family, who somehow were able to cope with the frustrations and the long absences, and whose unfailing devotion made all things happen.